

A Novel High Performance Magnetic Gear with Auxiliary Silicon Steel Sheet

Can Tan, and Libing Jing

Abstract—Magnetic gear is a transmission device with novel structure. It uses the principle of magnetic field modulation to transmit torque. In view of the magnetic leakage of the magnetic gear in the process of rotation and cannot be eliminated, a magnetic gear model with auxiliary silicon steel sheet is proposed. Based on the conventional magnetic gear structure, the silicon steel sheet is placed outside the permanent magnet of the outer rotor. The magnetization mode of the outer rotor permanent magnet is tangential magnetization, and the spoke structure is adopted, and the inner rotor PMs is surface mounted and magnetized in the radial magnetization. The improved model is simulated by finite element method under three-dimensional conditions, and the electromagnetic performances of the model are optimized. Compared with the conventional magnetic gear model, the improved model has good performance, which improves the transmission capacity of output torque and reduces torque ripple. It is a great significance to improve the performance of magnetic gear.

Index Terms—Magnetic gear, magnetic flux leakage, Magnetic field modulation, Magnetic flux density, Torque.

I. INTRODUCTION

As a kind of equipment widely used in industrial production, a mechanical gear has high transmission efficiency, high transmission power, and high reliability. However, during the rotation of mechanical gears, due to the meshing between the gears, there will be problems such as loss and noise. Therefore, it cannot be applied to occasions with high precision requirements. At the same time, in the process of mechanical gear use, it also needs to be regularly inspected and maintained, which increases the cost [1]. Magnetic gear is a kind of non-mechanical contact transmission device. It has the merits of low noise, low mechanical loss, and low processing cost [2]. Magnetic gears have become the most promising alternative to mechanical gears due to their high transmission ratio and high torque density.

With the deepening of research, the advantages of magnetic gear are becoming more and more obvious, but in the early

stages of the development of magnetic gears, their topological structure is single and most of the energy of PMs is wasted. At any moment, only a small part of PMs contribute to torque transmission, therefore, the development of magnetic gears is slow [3]. Until 2001, K. Atallah and D. Howe proposed a coaxial magnetic gear model (CMG) based on the principle of magnetic field modulation. The number of PMs of the inner rotor of the magnetic gear is 4 pairs of poles, and the number of PMs of the outer rotor is 22 pairs of poles. By making a prototype, the torque density of the model is $100\text{KN}\cdot\text{m}/\text{m}^3$ [4]-[5]. In order to obtain high torque density, rare permanent magnet materials, such as NdFeB, are used in magnetic gears. CMG fully utilizes the PMs on the inner and outer rotors, which increases the availability of the PMs, and supplements the deficiency of the conventional magnetic gear in torque [6]. Based on the principle of CMG model, different types of magnetic gear structures are proposed, such as harmonic magnetic gear, planetary magnetic gear, and linear magnetic gear [7]-[8]. In [9], a CMG magnetized by Halbach array is proposed, and its performance is analyzed. The research on CMG gradually changes from changing the topology to optimizing the parameters of CMG, and analyzes the torque output characteristics of the magnetic ring of magnetic gear under different shapes [10]. Reference [11] proposed a new CMG model, which contains two magnetic flux modulation rings, an inner and an outer magnetic flux modulation ring, and the results show that this model has the superiority of high torque. Reference [12] proposed and analyzed a new type of CMG containing high-temperature superconducting blocks; the inner rotor is an eccentric pole, and the outer rotor PMs are magnetized by the Halbach array. Its torque density can reach $173\text{KN}\cdot\text{m}/\text{m}^3$.

Although the above structure improves the torque density of the CMG, the leakage of energy emerged by the permanent magnet outside the rotor to the air is not considered. Due to the absence of insulating material, magnetic leakage cannot be avoided. These magnetic flux leakages are useless to improve the output torque. Therefore, so as to obtain higher output torque, we can improve the torque by using magnetic flux leakage.

In this paper, a magnetic gear with auxiliary silicon steel sheet is proposed. The output torque of the magnetic gear is improved by placing silicon steel sheet outside the outer rotor. The second section will introduce the structure of the model and theory. In the third part, the performance of the model is analyzed by finite element analysis (FEA). Finally, a conclusion is drawn in the fourth part.

Manuscript received December 09, 2021; revised February 08, 2022; accepted February 28, 2022. date of publication June 25, 2022; date of current version June 18, 2022.

This work was supported in part by National Natural Science Foundation of China and China Postdoctoral Science Foundation. ((Project No. 51707072, 2018M632855). (*Corresponding author: Libing Jing.*))

L. Jing, and C. Tan are with the College of Electrical Engineering and New Energy, China Three Gorges University, Yichang 443002, China (e-mail: jinglibing163@163.com).

Digital Object Identifier 10.30941/CESTEMS.2022.00027

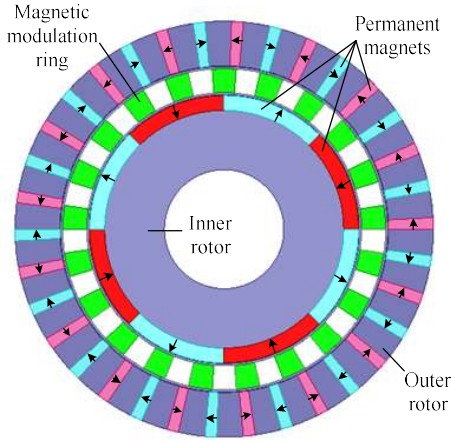


Fig. 1. Conventional CMG model.

II. STRUCTURE AND THEORY

As shown in Fig. 1, it is the structure of conventional CMG. Among them, those with more pole pairs are generally used as low-speed outer rotors, and those with fewer pole pairs are generally used as high-speed inner rotors. The magnetic regulating ring is composed of magnetic conducting steel and epoxy resin evenly distributed. These three parts rotate around the center O .

The CMG has two air gaps, the air gap between the inner rotor, the outer rotor, and the magnetic modulation ring is the inner air gap and the outer air gap, respectively. Between the two air gaps, the magnetic modulation ring plays a special role. It regulates the magnetic field generated by the PMs on the inner and outer rotors at the air gap, so that the magnetic fields can be coupled with each other and torque is transmitted.

After adding the magnetic modulation ring, the magnetic fields in the inner and outer air gaps are modulated to produce very rich harmonic components based on the original fundamental wave components. These harmonic components have their corresponding spatial pole pairs and specific speed in the air gap. The pole pairs of spatial harmonics contained in the air gap magnetic field of CMG can be expressed as

$$P_{m,k} = |mp + kn_s| \quad (1)$$

where $m=1, 3, 5, \dots, \infty$; $k=0, \pm 1, \pm 2, \dots, \infty$; p is the pole pairs of PMs on the inner rotor or outer rotor, n_s is the number of cores on the magnetic modulation ring. The relationship between n_s and p is satisfied

$$n_s = p_{in} + p_{out} \quad (2)$$

where p_{in} is the pole pair on the inner rotor, and p_{out} is the pole pair on the outer rotor.

The harmonic component has a specific spatial polar number and speed at the air gap, and the angular velocity of the harmonic component can be expressed as

$$\Omega_{m,k} = \frac{mp}{mp+kn_s} \Omega_r + \frac{kn_s}{mp+kn_s} \Omega_s \quad (3)$$

where $\Omega_{m,k}$ is the angular velocity of the harmonic component, Ω_r is the angular velocity of the inner or outer rotors, Ω_s is the angular velocity of the magnetic modulation ring.

When $k=0$, there are only inner rotor and outer rotor in the CMG. At this time, the spatial harmonic angular velocity is

equal to the rotor angular velocity. When $k \neq 0$, in addition to the inner and outer rotors, there are flux rings. At this time, the angular velocity of the spatial harmonic component needs to consider the influence of the angular velocity of the flux ring. The necessary condition for stable torque transmission of CMG is that the pole pairs of PMs on the two rotors are equal to the pole pairs of spatial harmonic components. When $m=1, k=-1$, at this time, except for the fundamental wave, the harmonic component is the largest spatial harmonic component, which can be expressed as

$$\Omega_{1,-1} = \frac{p}{p-n_s} \Omega_r - \frac{n_s}{p-n_s} \Omega_s \quad (4)$$

In practice, considering the stiffness and hardness of the magnetic modulation ring, the magnetic modulation ring is generally in a stationary state. Therefore, the gear ratio (G_r) of the CMG is

$$G_r = \frac{P_{out}}{P_{in}} \quad (5)$$

On the outer rotor of the magnetic gear, PMs and silicon steel sheets are distributed alternately to form a spoke structure. When rotating, part of the magnetic field of the PMs promotes torque transmission through silicon steel, and the other part leaks into the air to form magnetic flux leakage. By placing the silicon steel sheet on the outside of the outer rotor, the outer magnetic flux leakage can be returned through the silicon steel sheet, it can reduce the amount of magnetic flux leakage, thereby promoting torque transmission. The variation curve of silicon steel sheet and output torque under different depths and widths is shown in Fig. 2.

Fig. 2 shows the curve of the output torque of the CMG with the depth and width of the silicon steel sheet. It can be seen from the figure that after the silicon steel sheet is placed on the outside of the outer rotor, although the torques at different values are different, they all contribute to the increase of the output torque. When the depth of the silicon steel sheet is 0.8° and the depth is 1.75mm, the outer rotor has the maximum output torque.

The improved model is shown in Fig. 3, and its basic parameters are listed in Table I.

The difference between the improved model and the conventional model is that there is a layer of silicon steel outside the rotor permanent magnet of the improved model. Parallel magnetization can increase the torque. At the same

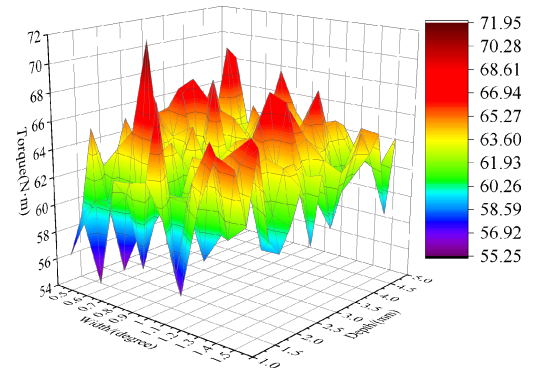


Fig. 2. Variation curve of output torque under different depth and width.

TABLE I
PARAMETERS OF IMPROVED CMG

Parameter	Value
Pole-pairs inner rotor	4
Pole-pairs outer rotor	17
The inner radius of the inner rotor yoke	20 mm
The outer radius of the inner rotor yoke	40 mm
Thickness of PMs	5mm
The outer radius of the stationary ring	54 mm
Thickness of the outer yoke	10 mm
The outer radius of the outer rotor yoke	70 mm
The length of the air gap	1 mm
Remanence of PMs	1.2T
Axial length	60 mm
Thickness of the air zone	15 mm
The width of silicon steel	0.8°
The length of silicon steel	1.75 mm
Number of outer silicon steel sheets	34

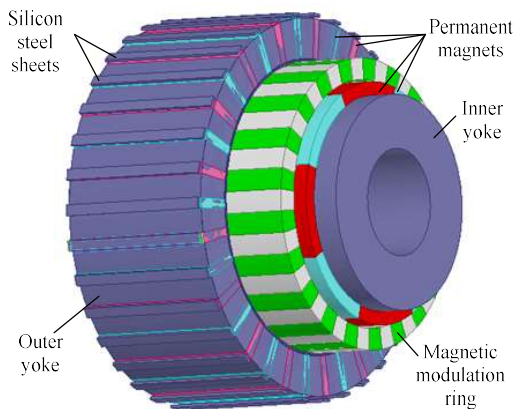


Fig. 3. Improved CMG model.

time, due to the alternating arrangement of PMs and silicon steel, the energy generated by the permanent magnet on the outer rotor will leak into the air, resulting in magnetic leakage and reducing the utilization efficiency of the permanent magnet. A layer of silicon steel sheet is added to provide a path for the outer magnetic flux leakage to circulate between the permanent magnet and the outer silicon steel, at the same time, the silicon steel sheet provides a return path with a smaller magnetic resistance for the magnetic field lines so that more magnetic leakage is used.

III. PERFORMANCES ANALYSIS

A. Magnetic Field

In order to make a good comparison between the two models, it is necessary to ensure that the basic parameters of the two models are the same, and compare the conventional and improved models by establishing a three-dimensional model.

Fig. 4 shows the distribution of magnetic dense clouds on the silicon steel sheet outside the improved model. It can be seen that some of the magnetic field energy leaked in the air is concentrated on silicon steel, which can be utilized. Fig. 5 shows the magnetic flux density distribution at the air gap.

The radial and tangential magnetic density waveforms of the inner air gap after finite element calculation are shown in Fig. 6. It can be seen from the figure that the radial amplitude component of the improved model is increased at the internal air gap, but it is the opposite in the tangential direction.

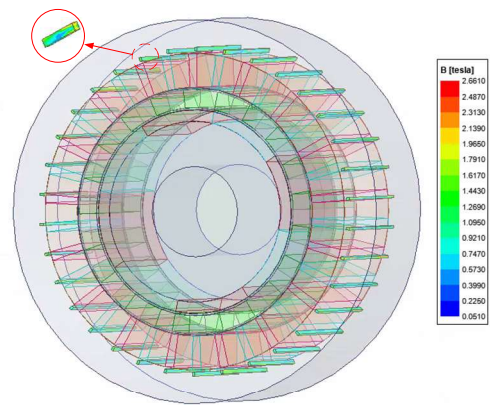


Fig. 4. Flux distribution of outer silicon steel.

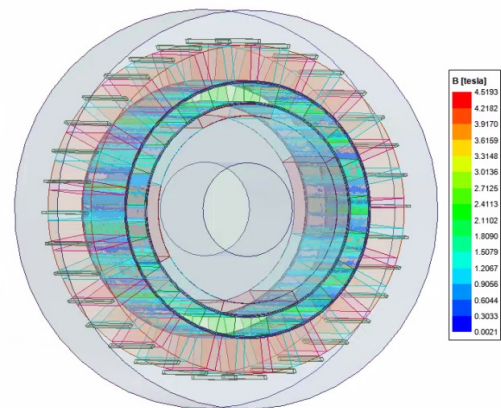


Fig. 5. Flux distribution at air gap.

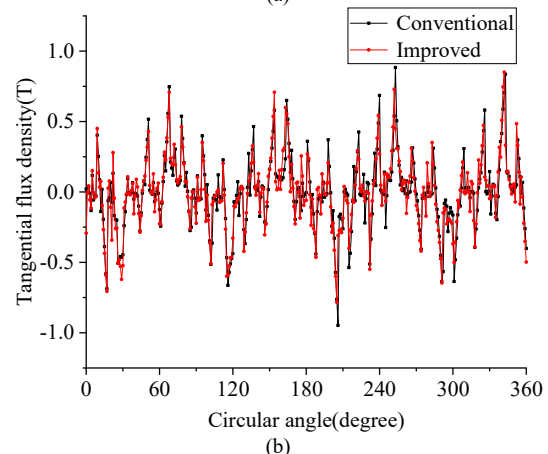
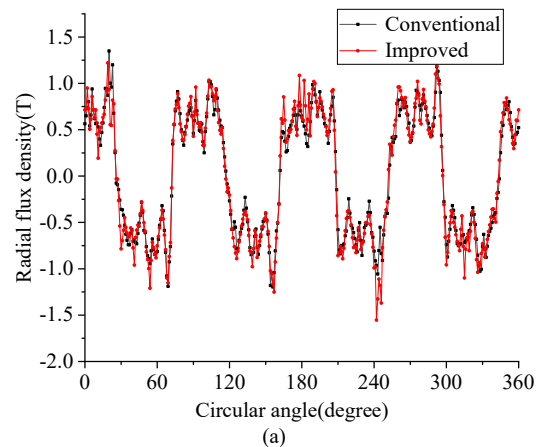


Fig. 6. Flux density distribution in the inner air gap: (a) Radial component. (b) Tangential component.

The corresponding harmonic spectra are shown in Fig. 7. In contrast to the conventional model, the 4th, 17th, and 25th harmonics are increased in the radial component, in the tangential component, the fundamental wave amplitude is increased, and the other harmonic amplitudes are slightly smaller than the conventional harmonic amplitudes.

Fig. 8 is the radial and tangential magnetic flux density waveforms of the two models in the external air gap. As can be seen from it that the air gap magnetic density amplitude of the improved model is greater than that of the conventional model.

The spectra after their decomposition are shown in Fig. 9. The 17th, 25th, and 38th harmonics are increased in both radial and tangential components. The 17th harmonic is the

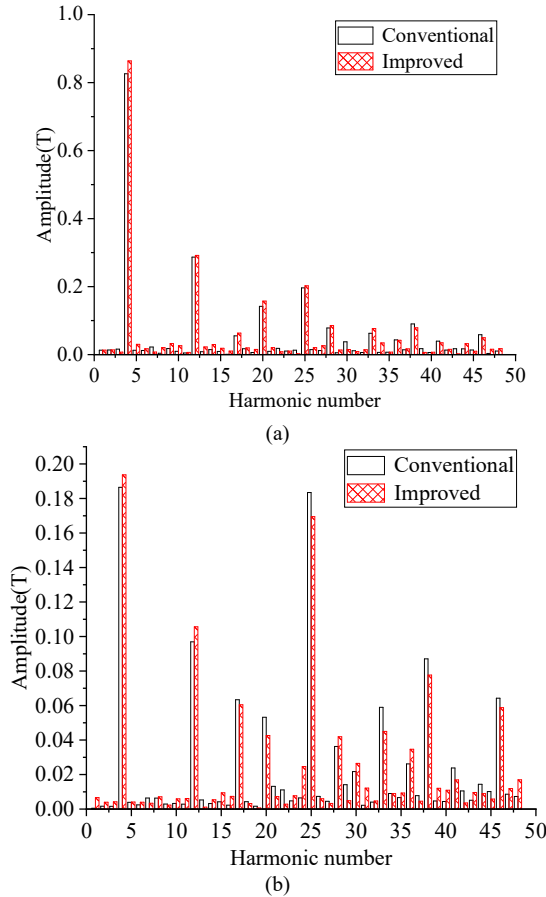
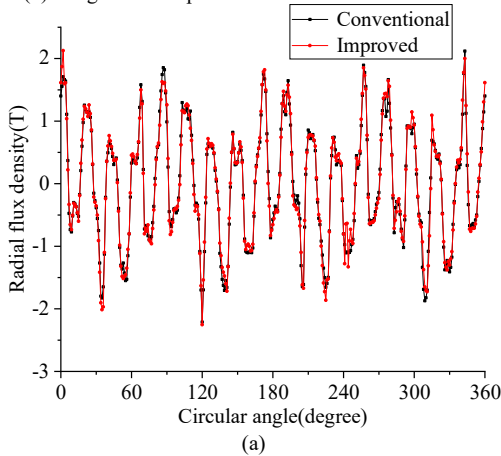
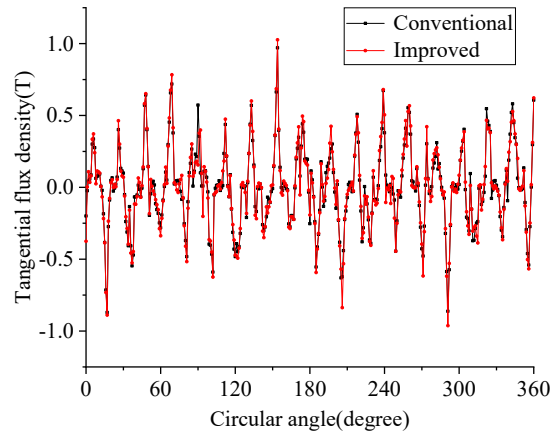


Fig. 7. Harmonic spectra of flux density in the inner air gap: (a) Radial component. (b) Tangential component.



(a)



(b)

Fig. 8. Flux density distribution in the outer air gap: (a) Radial component. (b) Tangential component.

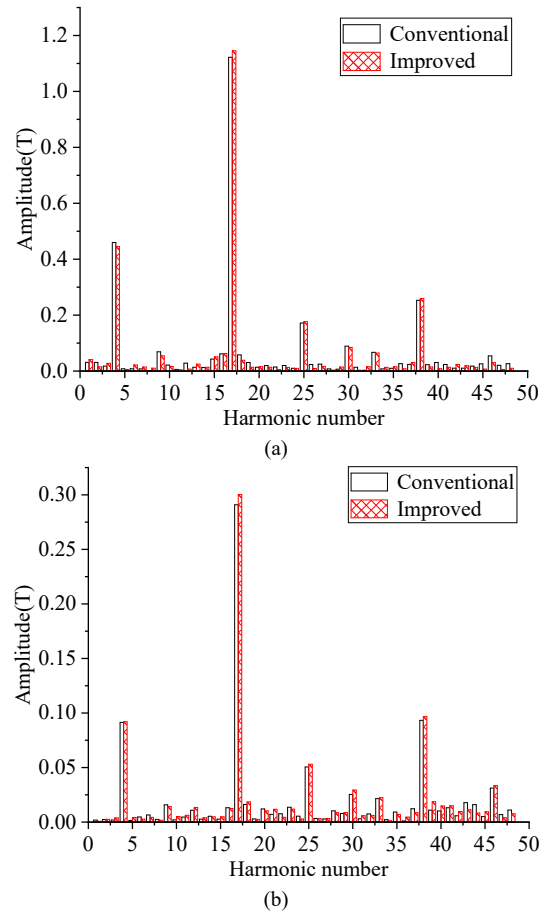


Fig. 9. Harmonic spectra of flux density in the outer air gap: (a) Radial component. (b) Tangential component.

fundamental harmonic in the outer air gap, and its amplitude is the largest. Increasing the amplitude of the 17th harmonic, which is helpful to improve the output torque of the outer rotor.

TABLE II. COMPARISON OF TORQUE RIPPLE BETWEEN CONVENTIONAL AND IMPROVED CMG

Type	T_{max} (N·m)	T_{min} (N·m)	T_{ave} (N·m)	$t\%$
Conventional	68.68	65.73	67.36	4.38
Improved	71.92	68.91	70.27	4.28

B. Torque

According to the Maxwell Stress tensor, the electromagnetic torque is expressed as follows

$$T_m = \frac{L_{ef} R_c^2}{\mu_0} \int_0^{2\pi} B_r B_\theta d\theta \quad (6)$$

where L_{ef} represents the effective value of the axial length of the CMG, μ_0 is the magnetic conductivity of the vacuum, R_e is the radius of the air gap, B_r and B_θ are the radial and tangential magnetic flux density, respectively.

Static torque indicates the maximum load that the CMG can bear, and it is one of the important indexes to investigate the performance of the CMG. The calculation of static torque is to fix one rotor and rotate the other. In this paper, the magnetic modulation ring and the outer rotor are stationary, and the inner rotor rotation speed is 170r/min, and the static torque waveform is shown in Fig. 10.

As can be seen from Fig. 10, the changes of torque and rotation angle are sinusoidal. When the circular angle is 98° , the inner rotor has the maximum static torque. The conventional and improved torque values are $18.09\text{N}\cdot\text{m}$ and $18.37\text{N}\cdot\text{m}$, respectively; and the torque is only increased by 1.55%. When the circular angle is 278° , the outer rotor has the maximum static torque. The torque values of the conventional model is $75.99\text{N}\cdot\text{m}$, and the torque values of the improved model is $79.32\text{N}\cdot\text{m}$, which increases by 4.38%.

When the magnetic modulation ring is fixed, the rotation speed of the inner rotor is 170r/min, and the rotation speed of the outer rotor is 40r/min, and it rotates in the opposite

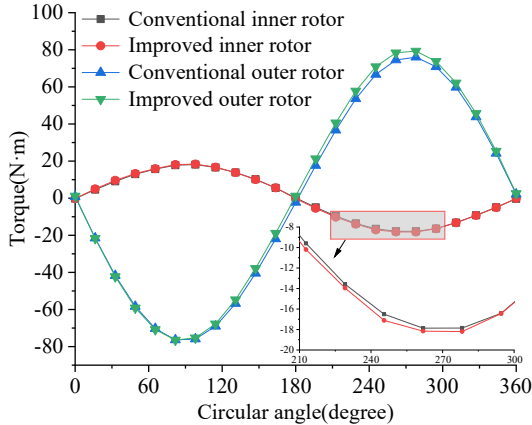


Fig. 10. Torque-angle curves.

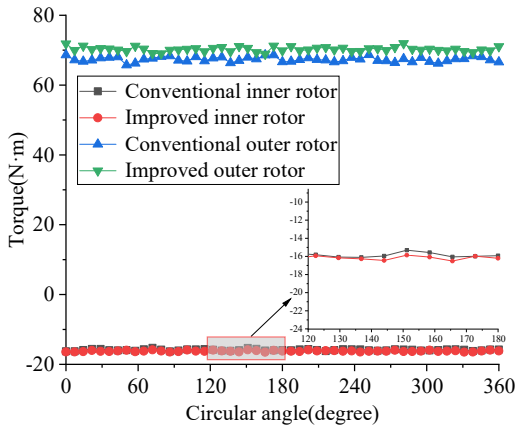


Fig. 11. Electromagnetic torque.

direction. Through simulation calculation, the electromagnetic torque curve is obtained, as shown in Fig. 11.

The fluctuation ranges of internal torque of the conventional model are $15.27\text{N}\cdot\text{m}$ to $16.28\text{N}\cdot\text{m}$, and the proposed model is $15.84\text{N}\cdot\text{m}$ to $16.50\text{N}\cdot\text{m}$. The fluctuation range of external torque is $65.73\text{N}\cdot\text{m}$ to $68.68\text{N}\cdot\text{m}$ and $68.91\text{N}\cdot\text{m}$ to $71.92\text{N}\cdot\text{m}$, respectively. Either from the perspective of the graph or the perspective of the data range, it can be seen that the internal and external torque of the improved model are greater than that of the conventional model. The average output torque is used for comparison, on the inner rotor, the output torque of the improved model is increased by 2.08% based on the traditional model; at the same time, on the outer rotor, based on the output torque of the conventional model, the output torque of the improved model increases by 4.32%.

Torque ripple is used to describe the stability of torque output. t is the torque ripple coefficient, and its expression is

$$t = \frac{T_{max} - T_{min}}{T_{ave}} \quad (7)$$

where T_{max} is the maximum value of output torque. T_{min} is the minimum value of output torque. T_{ave} is the average value of output torque. The size of t reflects the stability of torque output. The smaller the t value, the more stable the torque output.

Since the number of pole pairs of the PMs of the inner rotor is smaller than that of the PMs of the outer rotor, therefore, we pay more attention to the transmission stability of the output rotor, and at the same time, the reduction of magnetic flux leakage is helpful to improve the outer torque. While improving the output torque of the outer rotor, reducing the torque ripple of the outer rotor can improve the operation stability and improve the conveying efficiency. Table II shows the comparison of external rotor output torque ripple between the two models.

It can be seen from table II that the torque ripple of the improved model is reduced by 2.28% compared with the conventional model. The torque ripple of the model is reduced, and the stability of the output torque is improved, which contributes to the smooth transmission of torque.

IV. CONCLUSION

In this paper, a magnetic gear model with auxiliary silicon steel sheet to reduce magnetic flux leakage is proposed, which is analysed and calculated by the three-dimensional finite element method. The simulation results show that the improved CMG can change the amplitude of air gap magnetic density. The fluctuation range of internal torque is $15.84\text{N}\cdot\text{m}$ to $16.50\text{N}\cdot\text{m}$, and the fluctuation range of external torque is $68.91\text{N}\cdot\text{m}$ to $71.92\text{N}\cdot\text{m}$. By reducing magnetic flux leakage, the torque of CMG is improved. The output torque of the improved model is increased by 4.32% based on the output torque of the conventional model, reducing magnetic flux leakage is helpful to increase the utilization of PMs. At the same time, the torque ripple of CMG is analysed. The torque ripple of the improved model is 2.28% smaller than that of the conventional model. When the ripple is reduced, the torque output will be more stable.

REFERENCES

- [1] A. Leontaritis, A. Nassehi, and J. M. Yon, "A Monte Carlo Analysis of the Effects of Geometric Deviations on the Performance of Magnetic Gears," *IEEE Trans. Ind. Appl.*, vol. 56, no. 5, pp. 4857-4869, Sept.-Oct 2020.
- [2] L. B. Jing, J. Gong, and T. Ben, "Analytical Method for Magnetic Field of Eccentric Magnetic Harmonic Gear," *IEEE Access*, vol. 8, pp. 34236-34245, 2020.
- [3] L. B. Jing, Z. X. Huang, J. L. Chen, and R. H. Qu, "Design, Analysis, and Realization of a Hybrid-Excited Magnetic Gear During Overload," *IEEE Trans. Ind. Appl.*, vol. 56, no. 5, pp. 4812-4819, Sept.-Oct. 2020.
- [4] H. Y. Wong, J. Z. Bird, D. Barnett, and W. Williams, "A High Torque Density Halbach Rotor Coaxial Magnetic Gear," *IEEE International Electric Machines & Drives Conference*, pp. 233-239, 2019.
- [5] L. N. Jian, Z. X. Deng, Y. J. Shi, J. Wei, and C. C. Chan, "The Mechanism How Coaxial Magnetic Gear Transmits Magnetic Torques Between Its Two Rotors: Detailed Analysis of Torque Distribution on Modulating Ring," *IEEE/ASME Trans. Mechatronics*, vol. 24, no. 2, pp. 763-773, Apr. 2019.
- [6] A. Darabi, M. Abolghasemi, R. Mirzahosseini, and M. Sarvi-Maraghi, "Transient Analysis of an Axial Flux Magnetic Gear," *2020 28th Iranian Conference on Electrical Engineering*, pp. 1-5, 2020.
- [7] H. Zhao, C. H. Liu, Z. X. Song, and J. C. Yu, "A Fast Optimization Scheme of Coaxial Magnetic Gears Based on Exact Analytical Model Considering Magnetic Saturation," *IEEE Trans. Ind. Appl.*, vol. 57, no. 1, pp. 437-447, Jan. 2021.
- [8] K. Wang, Z. Y. Gu, Z. Q. Zhu, and Z. Z. Wu, "Optimum Injected Harmonics Into Magnet Shape in Multiphase Surface-Mounted PM Machine for Maximum Output Torque," *IEEE Trans. Ind. Electron.*, vol. 64, no. 6, pp. 4434-4443, Jun. 2017.
- [9] L. B. Jing, L. Liu, M. Xiong, and D. Feng, "Parameters Analysis and Optimization Design for a Concentric Magnetic Gear Based on Sinusoidal Magnetizations," *IEEE Trans. Appl. Supercond.*, vol. 24, no. 5, pp. 1-5, Oct. 2014.
- [10] S. J. Kim, E. Park, S. Jung, and Y. Kim, "Transfer Torque Performance Comparison in Coaxial Magnetic Gears With Different Flux-Modulator Shapes," *IEEE Trans. Magn.*, vol. 53, no. 6, pp. 1-4, Jun. 2017.
- [11] X. X. Zhang, X. Liu, and Z. Chen, "A Novel Dual-Flux-Modulator Coaxial Magnetic Gear for High Torque Capability," *IEEE Trans. Energy Convers.*, vol. 33, no. 2, pp. 682-691, Jun. 2018.
- [12] L. B. Jing, T. Zhang, Y. T. Gao, R. H. Qu, Y. H. Huang, and T. Ben, "A Novel HTS Modulated Coaxial Magnetic Gear With Eccentric Structure and Halbach Arrays," *IEEE Trans. Appl. Supercond.*, vol. 29, no. 5, pp.1-5, Aug. 2019.



Can Tan was born in Chongqing, China. He received his B.S degree in electrical engineering from Langfang Teachers College in 2020. He is currently working towards the M.S. in China Three Gorges University. His research interest includes electromagnetic field analysis design of magnetic gear and motor.



LiBing Jing was born in Henan province, China. He received his B.S degree from Zhongyuan University of Technology in 2006 and the Ph.D. degree from Shanghai University in 2013. Since July 2016, He has been an associate professor in the College of Electrical Engineering and New Energy, China Three Gorges University. Dr. Jing has authored over 90 published

technical papers and is the holder of over 10 patents/patent applications. He was recipient of the Best Poster Presentation Award from the 4th International Conference on Intelligent Green Building and Smart Grid (IGBSG 2019).

His research activities are related to design, modeling, and analysis of electrical machines.